Critical Velocity Correlations for Slurry Transport with Non-Newtonian Fluids

Subhash N. Shah and David L. Lord
Halliburton Services, Duncan, OK 73536

Transport properties of various uncross-linked and cross-linked non-Newtonian slurries in horizontal pipes are studied. Flow data are gathered in three long, different diameter, transparent horizontal pipes. Investigated are the effects of the pipe size, polymer concentration, fluid rheological properties, cross-linking effects, particle size and density, solids concentration, fluid density, and slurry rate on the critical deposition velocities and particle resuspension velocities. It is found that critical deposition and resuspension velocities for the non-Newtonian carrier fluids tested are significantly lower than those for water. Both velocities depend greatly on pipe size and particle density. Higher critical velocities are required to minimize settling (1) in larger pipe sizes and (2) for pumping solids denser than sand. For less viscous fluids, critical deposition and resuspension velocities increase slightly with increasing solids concentration. They are, however, independent of solids concentration for more viscous fluids.

Introduction

Extensive literature available from the slurry pipeline industry can be used to help the planner predict the critical deposition velocities of solids suspended in Newtonian fluids such as water, while being transported through horizontal pipes. No such information exists for estimating critical deposition velocities of solids transported through horizontal pipes in non-Newtonian carrier fluids. To quantify the solids transport capability of various non-Newtonian fluids, a laboratory investigation was initiated to experimentally determine critical deposition and resuspension velocities in horizontal pipe flow. This article reports the results of that investigation, which was conducted on pumping water and seven non-Newtonian fluids containing various particle types and sizes at concentrations ranging up to 0.31 volume fraction through three tubing sizes.

Based on their composite solid-liquid properties, slurries respond in a complicated way to imposed flow conditions. In fact, a broad range of flow behavior is possible depending on particular slurry properties and pipe flow conditions. Among the factors that must be considered are flow rate, pipe diameter and orientation, carrier fluid physical and rheological properties, and particle size, density and concentration. Two extremes of slurry behavior, homogeneous and heterogeneous flow, have been found to result from particular interactions of these factors as reported by Satchwell et al. (1988) and Wasp et al. (1977).

Homogeneous flow in a horizontal pipe is characterized by a uniform solids concentration across the pipe cross-section. A homogeneous slurry results when particle addition simply alters carrier fluid density and rheological characteristics. Solids addition to a very viscous carrier fluid or the addition of a high concentration of very fine particles to a thin carrier fluid usually produces a homogeneous slurry. The other extreme of slurry behavior in a horizontal pipe, heterogeneous flow is characterized by a pronounced solids concentration gradient with the highest concentration being along the pipe bottom. Heterogeneous slurries generally have lower solids concentration and/or larger particle sizes than homogeneous slurries.

Figure 1 shows typical wall shear stress vs. nominal shear rate responses for horizontal homogeneous and heterogeneous flow systems. At high nominal shear rate values, heterogeneous fluid response (curve A) tends to parallel homogeneous and/or carrier fluid response (curve B). As the heterogeneous slurry velocity decreases, the solids concentration gradient increases until either a stationary or slowly-moving particle bed appears along the pipe bottom. The slurry velocity at which a particle bed forms is defined as critical deposition velocity, V_D, and represents the lower pump rate limit for minimum particle

Correspondence concerning this article should be addressed to S. N. Shah.

settling. A further decrease in slurry velocity leads to increased friction loss, as indicated by a characteristic hook upward of curve A, and may also lead to pipe plugging. Slurries prepared with non-Newtonian carrier fluids are shown to exhibit this heterogeneous response, as will be discussed later.

If shut-down occurs while pumping a heterogeneous slurry, solids will be deposited in a stationary bed along the pipe bottom. At some point following such a shut-down, it will become necessary to resuspend these solids to remove them from the pipe. If flow rate over the settled solids is gradually increased, a response similar to curve A of Figure 1 is once again obtained. With increasing nominal shear rate, wall shear stress decreases until a minimum is reached and then increases rapidly thereafter. The fluid velocity that corresponds to this minimum stress value is the critical resuspension velocity, V_s. Experimental results reported later show that V_s is generally larger than V_D.

Curve B shows the expected response of a homogeneous slurry. This response is similar to carrier fluid behavior. At high nominal shear rate values, there is a steep linear turbulent flow regime. As slurry velocity decreases in the turbulent regime, a sudden transition to a flat laminar flow regime is seen to occur. The transition velocity, V_T, corresponds to this change in flow regimes and remains the same whether approached from turbulent or laminar flow directions. While slurries considered here are heterogeneous, their non-Newtonian carrier fluids give a homogeneous laminar flow response, which can be characterized by Power law parameters n and K. The apparent viscosity, μ_a, defined with these parameters, is used with other fluid and particulate properties to correlate experimentally-determined critical deposition and resuspension velocities.

Oroskar and Turian (1980) developed a critical deposition velocity correlation based on balancing energy required to suspend particles with energy dissipated by an appropriate fraction, χ, of turbulent eddies present in the flow. They estimated χ based on the assumption that only those eddies possessing instantaneous velocities equal to or greater than the hindered settling velocity are effective in maintaining particles in suspension. They found χ to be usually very close to unity (>0.95) and therefore its inclusion, especially when raised to a fractional power, has essentially no influence on correlation predictions. Their equation appears in the following form:

$$\frac{V_D}{\sqrt{gd\ (s-1)}} = 1.85C^{0.1536}(1-C)^{0.3564} \times (d/D)^{-0.378}\tilde{N}_{Re}^{0.09}\chi^{0.30} \quad (1)$$

Parameters appearing in Eq. 1 are defined in the Notation section. Their inclusion in this equation is based on analytical considerations while coefficient and exponent values were obtained from regression analysis of 357 critical velocity data sets. These data were extracted from a number of experimental investigations reported in the literature. Oroskar and Turian also provide an excellent review and evaluation of other critical velocity correlations appearing in the following literature: Durand (1952), Kao and Wood (1974), Newitt et al. (1955), Spells (1955), Turian and Yuan (1977), Wasp et al. (1977), and Zandi and Govatos (1967). Using turbulence theory, Davies (1987) was able to deduce a simple theoretical justification for the empirically derived exponents of Eq. 1.

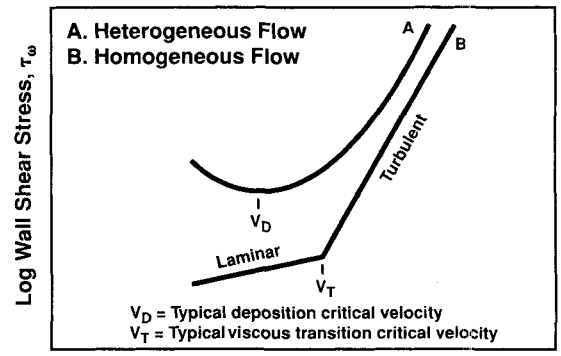

Figure 1. Wall Shear Stress vs. Nominal Shear Rate for Homogeneous and Heterogeneous Slurries

The Oroskar-Turian correlation and others appearing in the literature were all developed to describe critical deposition velocity of Newtonian carrier fluids with various solid types, sizes and concentrations. The authors are not aware of any such correlation for non-Newtonian carrier fluids nor for the resuspension phenomena associated with either Newtonian or non-Newtonian fluids. In the absence of adequate theory for description of these phenomena, Eq. 1 was generalized to increase its capability to correlate critical velocity measurements with specific operating conditions. The parameter χ was eliminated from the generalization because of its insignificant contribution to the correlation results and because it would be undefined for the laminar flows associated with many of the non-Newtonian fluid measurements. The generalized form of Eq. 1, which can be applied to either critical deposition or resuspension velocity, is as follows:

$$\frac{[V_D] \text{ or } [V_s]}{\sqrt{gd\ (s-1)}} = YC^{0.1536}(1-C)^{0.3564}(d/D)^{-w}\tilde{N}_{Re}^{z} \quad (2)$$

where coefficient Y, and exponents w and z are adjustable constants that can be evaluated by regression analysis for particular critical velocity data sets. Apparent viscosity, μ_a, is substituted into the modified Reynolds number expression $\tilde{N}_{Re}$, of Eq. 2 to further generalize Eq. 1 to non-Newtonian fluids.

Equipment and Procedure

A schematic diagram of the experimental setup is provided in Figure 2. Principal components shown are three different diameter polycarbonate tubes, a 208.2-dm^3 fluid mixing vessel, progressive cavity pump, differential pressure transducer, flowmeter, temperature probe, video camera, and two concentric-pipe heat exchangers. The three horizontal flow tubes have 3.18-mm wall thickness and have outside diameters of 3.81, 5.72 and 6.99 cm, respectively. Each flow conduit was assembled from seven 2.4-m sections using special clamps to provide an overall 16.8-m length. Each flow conduit was tapped with four 1.59-mm holes to facilitate differential pressure measurements across 4.57-, 9.14- and 13.72-m lengths. The first pressure tap is located 1.83 m from the entrance and the last tap is located 1.22 m from the exit of each flow conduit.

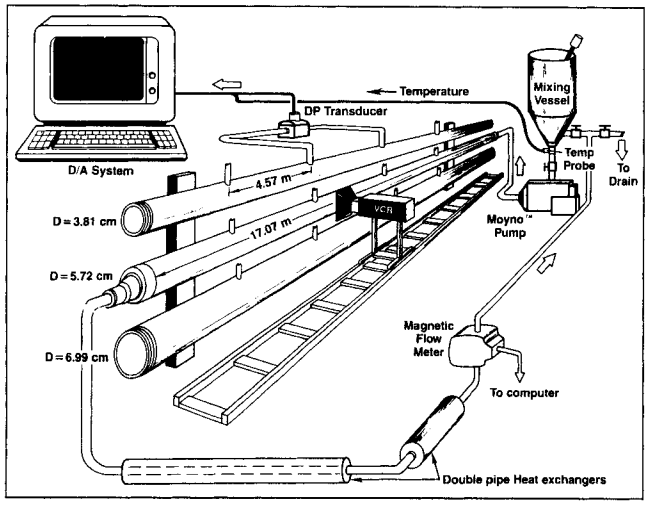

Figure 2. Experimental Setup of Slurry Transport in Horizontal Pipes

A magnetic flowmeter of 3.81-cm ID was placed vertically on the downstream side to monitor slurry flow rate.

Test fluids were mixed to the desired concentrations in a mixing vessel equipped with a double, three-bladed impeller air mixer. Mixing vessel fluid temperature was monitored and adjusted to maintain approximately isothermal conditions using the concentric-pipe heat exchangers. To ensure complete solids suspension in the return line to the mixing vessel, a diameter smaller than the three horizontal flow conduits was selected.

Fluid and solids movements in the transparent flow conduits were monitored and recorded with a video camera installed on a specially designed stand and track system that allowed the camera to travel axially along each tube.

Table 1 provides a list of various slurries used for testing in all three pipes. Newtonian slurries prepared using fresh water containing 20–40 U.S. Mesh sand at concentrations of 0.044, 0.084, 0.12 and 0.15 volume fractions were used to check and calibrate the system. When using sand, a few black India-ink-coated grains were added to uncoated sand to improve visualization of fluid and solids motion in the tubing.

Non-Newtonian fluids were initially prepared without solids and their steady-state differential pressure measured at various decreasing flow rates. Solids at 0.15 volume fraction were then added while circulating at a high flow rate to prevent settling along the flow conduit bottom. Steady-state differential pressure vs. flow rate data were then gathered with slurry at decreasing flow rates. A video recording of slurry motion at each decreasing flow rate was also made for later analysis. Upon completing the series of decreasing flow rates, slurry flow rate was then gradually increased while gathering differential pressure vs. flow rate data to detect resuspension of the settled bed. While circulating at high rate, additional solids were then mixed to prepare the next slurry concentration. Testing then proceeded with the new slurry concentration in the same manner as just described for 0.15 volume fraction slurry. These steps were repeated until all solids concentrations were evaluated according to the schedule provided in Table 1. It should be mentioned here that while obtaining data, all slurries were continuously recirculated through the flow loop. Because of this, there might have been some change in the rheological characteristics of the carrier fluids.

Results and Discussion

For each slurry tested, differential pressure, Δp, vs. flow rate, Q, was first converted in terms of wall shear stress, τ_w and nominal shear rate, γ. Then, a logarithmic plot of τ_w vs. γ (similar to curve A in Figure 1) was prepared for each slurry, and critical deposition or resuspension velocity corresponding to minimum wall shear stress was determined. Data recorded by video camera, visual observations made while testing slurry, and pressure drop vs. time data were also considered in determining these critical velocities. From these critical velocities, critical flow rates could be determined.

Experimental critical deposition and resuspension velocities thus determined for sand/water slurries were compared to the more generalized and well-accepted Eq. 1. However, it was found necessary to modify Eq. 1 for non-Newtonian slurries to better match the experimental data.

For data analysis, the internal diameters of the three tubes were determined by pumping fresh water in turbulent flow at various flow rates and gathering Δp vs. Q data. These data

Table 1. Particle Type and Volume Fraction Solids Used

Fluid Tested	3.81 cm	5.72 cm	6.99 cm
Fresh Water	0.044*, 0.084, 0.12, 0.15 20–40 sand	0.044, 0.084, 0.12, 0.15 20–40 sand	0.044, 0.084, 0.12, 0.15 20–40 sand
1.2 kg/m^3 HPG	0.15, 0.21, 0.27 20–40 sand	0.15, 0.21, 0.27 20–40 sand	0.15, 0.21, 0.27, 20–40 sand
2.4 kg/m^3 HPG	0.15, 0.21, 0.27 20–40 sand	0.15, 0.21, 0.27 20–40 sand	0.15, 0.21, 0.27 20–40 sand
4.8 kg/m^3 HPG	0.15, 0.27, 0.31 20–40 sand	0.15, 0.27, 0.31 20–40 sand	0.15, 0.27, 0.31 20–40 sand
	—	—	0.15, 0.26, 0.30 16–20 LWC**
	—	—	0.13, 0.23, 0.27 16–20 HWC†
7.2 kg/m^3 HPG	0.15, 0.27, 0.31 20–40 sand	0.15, 0.27, 0.31 20–40 sand	0.15, 0.27, 0.31 20–40 sand
4.8 kg/m^3 cross-linked HPG	0.15, 0.27, 0.31 20–40 sand	0.15, 0.27, 0.31 20–40 sand	0.15, 0.27, 0.31 20–40 sand
	—	—	0.15, 0.26, 0.30 16–20 LWC
	—	—	0.13, 0.23, 0.27 16–20 HWC
7.2 kg/m^3 cross-linked HPG Polymer emulsion‡	0.15, 0.27, 0.31 20–40 sand	0.15, 0.27, 0.31 20–40 sand	0.15, 0.27, 0.31 20–40 sand
	—	—	0.15, 0.27, 0.31 20–40 sand
	—	—	0.13, 0.27 16–20 HWC

*volume fraction solids
**Light weight ceramic—specific gravity 2.75
†Heavy weight ceramic—specific gravity 3.25
‡67:33 oil:water ratio, 4.8 kg hydroxyethylcellulose (HEC)/m^3 in water

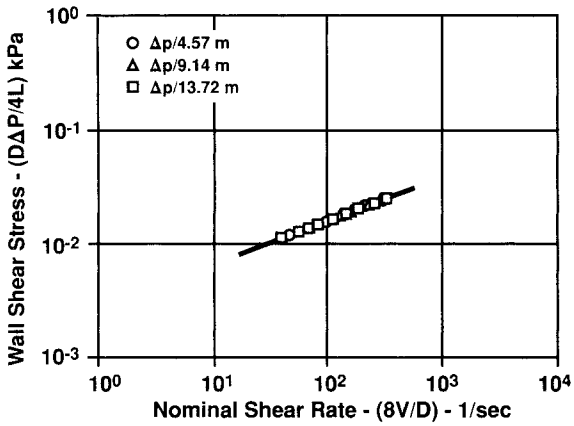

Figure 3. τ_ω **vs.** γ **for 7.2 kg/m³ HPG Fluid in 6.99 cm Pipe**

were converted in terms of Fanning friction factor, f, and Reynolds number, N_{Re}, and compared with the Newtonian equation for turbulent flow. The diameter giving the best fit of experimental data with the theoretical equation was considered to be the internal diameter of the tubing. Internal diameters determined hydraulically were generally in good agreement with internal diameters reported by the manufacturer.

For fluids without solids, Δp vs. Q data were converted to obtain wall shear stress, τ_w, and nominal shear rate, γ. A logarithmic plot of τ_w vs. γ was prepared for each fluid. Figure 3 depicts such a plot for 7.2 kg/m³ hydroxypropyl guar (HPG) fluid in 6.99-cm tubing. The Δp data gathered from all three lengths of 6.99-cm tubing show excellent agreement.

A similar τ_w vs. γ plot, but with data from three tubes, is shown in Figure 4 for 4.8-kg/m³ cross-linked HPG fluid. Considering that three separate polymer solution batches were prepared (one for each tube) and that cross-linking with each polymer solution occurs separately, the agreement is very good.

Laminar flow data collected in all three tubes with fluid containing no solids were combined (as shown in Figure 4) for analysis. The experimental τ_w vs. γ data were then fitted with the following Power law model:

$$\tau_w = K(\gamma)^n \tag{3}$$

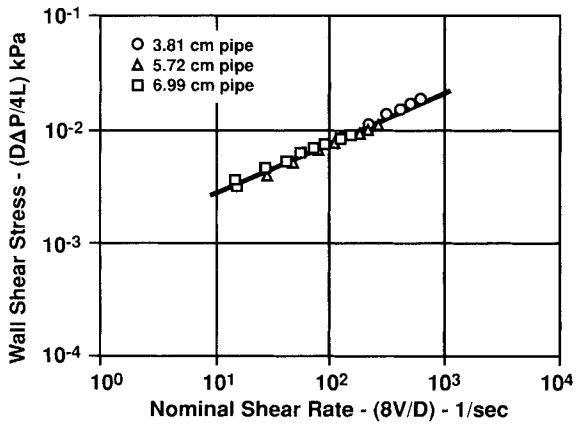

Figure 4. τ_ω **vs.** γ **for 4.8 kg/m³ Cross-linked HPG Fluid in Three Pipes**

Table 2. Rheological Properties and Model Parameters of Fluids Tested at 26.7°C

Fluid	n	K(Pa·s^n)	y	w	z
1.2 kg/m³ HPG	0.941	0.00488	3.4260	0.6696	−0.1481
2.4 kg/m³ HPG	0.719	0.0546	2.2573	0.4691	0.0294
4.8 kg/m³ HPG	0.486	0.6942	0.1743	0.4830	0.5276
7.2 kg/m³ HPG	0.377	2.7195	0.2360	0.4513	0.4274
4.8 kg/m³ cross-linked HPG	0.446	0.9719	0.0639	0.3786	0.7858
7.2 kg/m³ cross-linked HPG	0.304	4.3091	0.0613	0.4356	0.6476
Polymer emulsion	0.516	2.9733	0.2075	−0.067	1.0297

and from regression analysis, the values of constants n and K were obtained. These results are presented in Table 2.

A typical plot of Δp and Q vs. elapsed time for slurries is depicted in Figure 5. The plotted data are for 4.8-kg/m³ HPG fluid containing 0.31 volume fraction 20–40 mesh sand in 6.99-cm pipe. It can be seen in Figure 5 that as flow rate decreased, differential pressure decreased as expected up to a certain critical flow rate. As rate decreased beyond this critical flow rate, the particles slowly migrated to the tubing bottom, creating a stratified flow or concentration gradient across the vertical axis of the pipe. The particle deposition reduced the flow area, which in turn resulted in higher differential pressures.

The second half of Figure 5 shows the effect of increasing flow rate on differential pressure. As the flow rate increased, the particles were gradually resuspended in the main core of the slurry, thus increasing the effective diameter of the pipe, which in turn resulted in lower Δp values. The Δp decreased up to a certain critical resuspension flow rate at which all particles were resuspended, and beyond this rate Δp increased as rate increased.

For each slurry the Δp values were monitored across 4.57, 9.14 and 13.72 m. With some slurries, slight differences in Δp from the three tube lengths were noticed, while in other cases there were no appreciable differences. However, for those cases where Δp values from all three sections were different, critical deposition and resuspension flow rates computed individually from each of the three sets had approximately the same value.

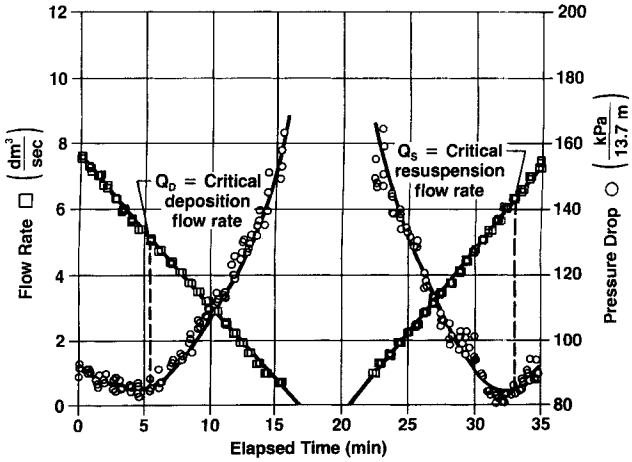

Figure 5. Differential Pressure and Flowrate vs. Elapsed Time

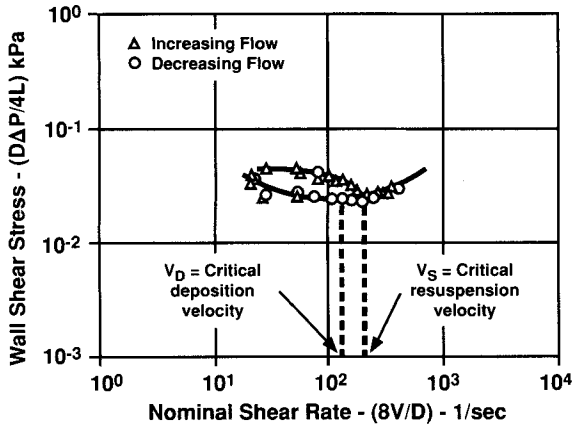

Figure 6. τ_ω vs. γ for 4.8 kg/m^3 Cross-linked HPG Fluid Containing 0.27 Volume Fraction 20-40 Sand in 5.72 cm Pipe

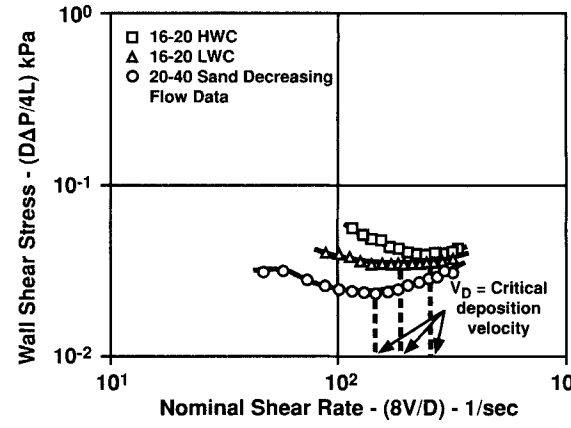

Figure 8. τ_ω vs. γ for 4.8 kg/m^3 Cross-linked HPG Fluid Containing 0.31 Volume Fraction Solids in 6.99 cm pipe

Therefore, in the analysis of critical flow rates for all slurries, the differential pressures across the 13.72-m length were used.

Figure 6 shows a typical plot of τ_w vs. γ for a given slurry. The data presented are for the 4.8-kg/m^3 cross-linked HPG fluid containing 0.27 volume fraction 20–40 mesh sand in a 5.72-cm pipe. The increasing as well as decreasing flow rate data are presented. First, decreasing flow rate data were gathered to determine critical deposition velocity, and increasing flow rate data were then gathered to determine critical resuspension velocity. When decreasing flow rate data of Figure 6 is compared with curve A of Figure 1, it is clear that the slurry tested is a heterogeneous, not a homogeneous, slurry. Similar plots were obtained with all other slurries.

Nominal shear rates corresponding to minimum wall shear stresses for both decreasing and increasing flow rate curves were determined (see Figure 6). From these nominal shear rates, critical deposition and resuspension velocities were calculated. Above the critical deposition velocity, particles were completely suspended and no bed was deposited along the pipe bottom. At the critical velocity, many of the particles settle to the bottom and stratification becomes evident. The particle bed formed along the pipe bottom was stagnant for sand/water slurries, while for non-Newtonian slurries it was in motion at the critical velocity. Below critical deposition velocity the deposited bed for sand/water slurries was packed and stagnant, while for non-Newtonian slurries it was loosely packed and still moving, although movement was slow compared to fluid above the bed.

It should be noted from Figure 6 that while gathering increasing flow rate data, the wall shear stress values are substantially higher than the decreasing flow rate data. The reasons for this may be because slurry transport in horizontal pipes is a time-dependent phenomenon. With time, more solids are deposited, thus compacting the semisettled bed and further reducing the area available for fluid to flow. As the rate is increased, the particles are being picked back up into the main fluid core, and differential pressures or wall shear stress values decrease. Once all particles are in resuspension, i.e., above the critical resuspension velocity, the wall shear stress increases as the flow rate increases.

Effect of gel concentration on the critical deposition velocity is demonstrated in Figure 7. The τ_w vs. γ data are presented for 4.8- and 7.2-kg/m^3 HPG fluids containing 0.31 volume fraction 20–40 mesh sand in a 3.81-cm tubing. As expected, the higher viscosity of a 7.2-kg/m^3 fluid, compared to a 4.8-kg/m^3 fluid, allows particles to stay in suspension longer and results in a lower critical deposition velocity.

Particle density effect on critical deposition velocity is depicted in Figure 8. The τ_w vs. γ data of 4.8-kg/m^3 cross-linked HPG fluids containing 0.31 volume fraction sand and two different specific gravity ceramic particles in a 6.99-cm pipe are presented. Figure 8 shows that critical deposition velocity increases as the particle density increases. A higher critical velocity is required for the slurry prepared with particles denser than sand. Further, it should be noted from Figure 8 that the difference in critical deposition velocity of sand slurry vs. a light weight ceramic particle (LWC) slurry is significant even though their specific gravities do not differ significantly. This result is probably caused by particle size variation, since the sand slurry is prepared with 20–40 mesh particles while the LWC slurry is prepared with 16–20 mesh particles.

To compare the experimental data with model predictions, we first calculated the percent deviation between experimental data points and theoretical correlation prediction by the following equation:

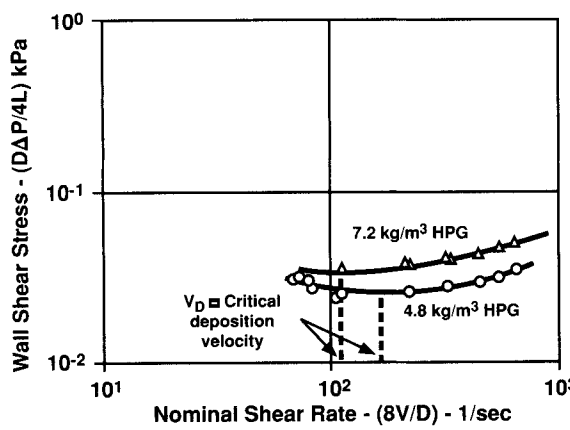

Figure 7. τ_ω vs. γ for 4.8 kg/m^3 and 7.2 kg/m^3 HPG Fluids Containing 0.31 Volume Fraction 20-40 Sand in 3.81 cm Pipe

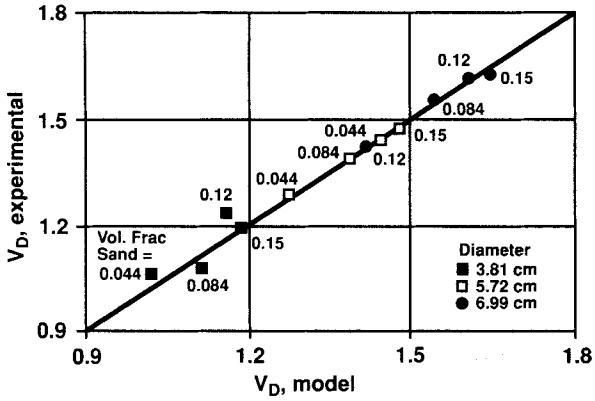

Figure 9. Critical Deposition Velocity Correlation for Sand/Water Slurries

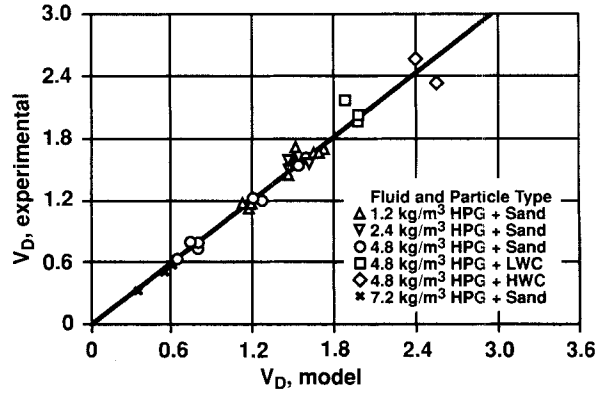

Figure 10. Critical Deposition Velocity Correlation for Slurries Prepared with Uncross-linked Fluids

$$\% \text{ deviation} = D_v = \left[\frac{V_{D,\text{model}} - V_{D,\text{exp}}}{V_{D,\text{exp}}}\right] \times 100 \qquad (4)$$

From these percent deviations, an overall percent root mean square deviation was then calculated as follows:

$$\% \text{ rms deviation} = \left[\sum_{i=1}^{N} D_v^2/N\right]^{1/2} \qquad (5)$$

Experimental critical deposition velocities of sand/water slurries containing 0.044, 0.084, 0.12 and 0.15 volume fraction 20–40 mesh sand in all three tubes are compared in Figure 9 with Eq. 1. The experimental data are in excellent agreement with the predictions of Oroskar and Turian (1980) with a percent rms deviation of 2.65 (see Table 3).

The best match of experimental critical resuspension velocities of sand/water slurries was obtained by altering the constants Y and z in Eq. 2. These values for sand/water slurries are $Y = 0.948$ and $z = 0.181$. Agreement between experimental data and model predictions was again excellent with a percent rms deviation of 2.64. As expected, all critical resuspension velocities obtained were higher than the corresponding critical deposition velocities.

For non-Newtonian fluids, correlations for polymer solutions and cross-linked fluids were derived independently. Both correlations employed the same basic form of Eq. 2. The constants Y, z, and w in Eq. 2 were obtained from regression analysis. Experimental critical deposition velocities for 1.2, 2.4, 4.8 and 7.2 kg/m^3 HPG fluids containing sand and ceramic particles are compared with the predicted values from the model in Figure 10. The experimental data are in excellent agreement with the model prediction. A similar comparison is also made with critical resuspension velocity data, which also agreed with predicted values very well (see Table 3 containing individual percent rms deviation values). Most resuspension velocities were in the range of 15% to 50% greater than their corresponding deposition velocities except for the most viscous fluids (7.2 kg/m^3 cross-linked HPG and polymer emulsion fluids to be discussed later), where resuspension velocities were two to three times depositional velocities. The depositional velocities of the latter fluids, however, are very small, and a two- to threefold increase in their value would still produce resuspension velocities smaller than the values for the other fluids.

The correlation to predict critical deposition and resuspension velocities for cross-linked fluid was developed by employing data gathered with 4.8 and 7.2 kg/m^3 cross-linked HPG slurries. Again, the parameters, Y, w, and z were obtained from the regression analysis. Figure 11 shows the match of experimental critical resuspension velocity data with model predictions for all cross-linked fluids studied, which again is in reasonably good agreement. The percent rms values for the critical resuspension velocity data are listed in Table 3.

Table 3. Statistical Evaluation of Critical Deposition and Resuspension Velocity Data

	% RMS Deviation	
Fluid	Deposition	Resuspension
Water	2.65	2.64
1.2 kg/m^3 HPG	4.48	3.58
2.4 kg/m^3 HPG	2.88	3.69
4.8 kg/m^3 HPG	5.76	9.68
7.2 kg/m^3 HPG	4.14	4.65
4.8 kg/m^3 cross-linked HPG	9.54	9.40
7.2 kg/m^3 cross-linked HPG	15.14	7.79
Polymer emulsion	7.01	2.88

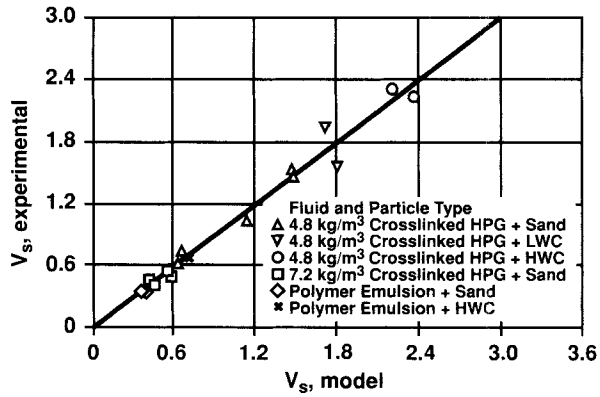

Figure 11. Critical Resuspension Velocity Correlation for Slurries Prepared with Cross-linked Fluids

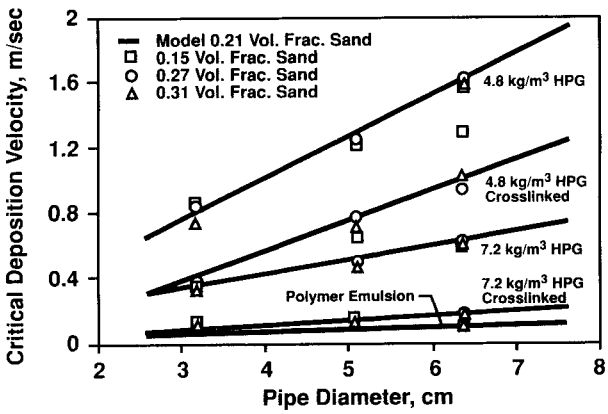

Figure 12. Effect of Pipe Diameter on Critical Deposition Velocity

In Figure 12, experimental critical deposition velocities from three pipes are compared to model predictions based on the parameters listed in Table 2 for cross-linked and uncross-linked 4.8 and 7.2 kg/m^3 HPG fluids containing various volume fractions sand. This figure shows that critical deposition velocity is very dependent on pipe size, particularly for the less viscous fluids. Similar trends for resuspension velocities as a function of pipe diameter were noted. Though not shown in Figure 12, critical velocities for 1.2 kg/m^3 HPG slurries were essentially the same as those for water while critical velocities for 2.4 kg/m^3 HPG slurries were slightly lower and parallel to those for water. Critical velocities of other, more viscous, non-Newtonian slurries were substantially lower than those for sand/water slurries. In turn, critical velocities for cross-linked slurries were substantially lower than their uncross-linked counterparts. Figure 12 also shows that particle concentration has little effect on the experimental depositional velocities. In fact, for the most viscous slurries, the critical velocities are essentially independent of particle concentration.

In Figure 13, experimental critical deposition velocities for three fluids of varying viscosity are shown plotted as a function of particle to fluid density ratios. Since critical resuspension velocity follows these same trends, it is clear that as particle density increases, greater velocities are needed (1) to avoid settling and (2) to resuspend settled particles.

In the present study, most of the critical depositional velocities correspond to laminar or near-laminar flow conditions based on a critical value of 2,100 for the Dodge-Metzner (1959) generalized Reynolds number. In this definition of Reynolds number, power-law apparent viscosity is substituted for viscosity in the usual expression for pipe flow. Test conditions selected for calculation of generalized Reynolds number values shown in Table 4 provide the maximum values encountered during experimentation. Selected conditions provide maximum values because the largest critical velocities occur in the largest tubing. Where data were available, calculations for heavier particles were also included in Table 4. Generalized Reynolds number values correspond to laminar or transition flow conditions, except for water and low concentrations of HPG.

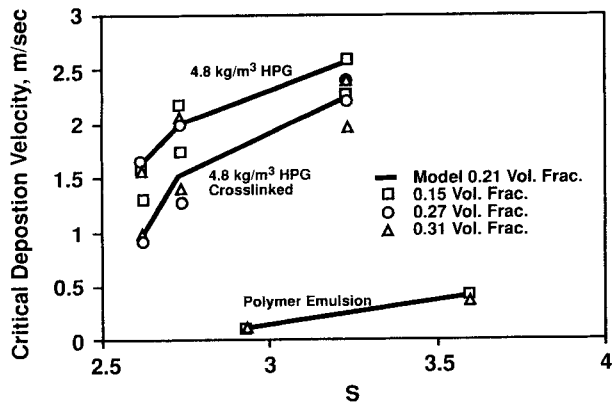

Figure 13. Effect of Particle Density on Critical Deposition Velocity for 6.99 cm Pipe

Table 4. Carrier Fluid Reynolds Numbers at the Critical Deposition Velocity in 6.99-cm Pipe for 0.15 Volume Fraction Solids

	V_D (m/s)		N_{Re}	
Fluid	Sand	HWC*	Sand	HWC*
Water	1.66	—	120,000	—
1.2 kg/m^3 HPG	1.65	—	29,500	—
2.4 kg/m^3 HPG	1.59	—	8,210	—
4.8 kg/m^3 HPG	1.59	2.59	2,230	4,650
7.2 kg/m^3 HPG	0.60	—	210	—
4.8 kg/m^3 cross-linked HPG	1.31	2.29	1,450	3,450
7.2 kg/m^3 cross-linked HPG	0.16	—	19	—
Polymer emulsion	0.10	—	6.5	—

*HWC = heavyweight ceramic

Conclusions

- An apparatus has been designed and assembled to study transport properties of various non-Newtonian slurries in horizontal pipes. Experimental critical deposition and resuspension velocity data have been gathered.
- It is found that critical deposition and resuspension velocities for non-Newtonian fluids tested are significantly lower than those for water.
- Both critical deposition and resuspension velocities depend greatly on pipe size. Higher critical velocities are required in larger pipe sizes to minimize settling.
- Higher critical deposition and resuspension velocities are required for particles denser than sand.
- For less viscous fluids, critical deposition and resuspension velocities increase slightly with increasing solids concentration. They are, however, independent of solids concentration for more viscous fluids.

Acknowledgment

We would like to thank Halliburton Services management for permission to publish this article and to the technical and secretarial staff for their assistance. We would also like to extend our appreciation to the reviewers who provided many valuable comments and suggestions for the revision of this article.

Notation

C = solids concentration, volume fraction
d = diameter of particle
D = diameter of pipe

D_v = percent deviation Eq. 4
f = Fanning friction factor, $f = D\Delta p/2L\rho_f v^2$
g = acceleration due to gravity
K = consistency index, Power law model constant
L = length of pipe
n = flow behavior index, Power law model constant
N_{Re} = Reynolds number $Dv\rho_f/\mu$ or $Dv\rho_f/\mu_a$
$\tilde{N}_{Re}$ = modified Reynolds number, $[D\rho_f\sqrt{gd(s-1)}]/\mu$ or μ_a
Δp = pressure drop or friction pressure
Q = flow rate
s = ratio of particle to fluid densities, ρ_p/ρ_f
t = time
v = mean slurry velocity
V_D = critical deposition velocity
V_s = critical resuspension velocity
w = constant in Eq. 2
Y = constant in Eq. 2
z = constant in Eq. 2

Greek letters

γ = nominal shear rate, $\gamma = 8v/D = 32Q/\pi D^3$
μ = viscosity of Newtonian fluid
μ_a = apparent viscosity of Power-law fluid, $\mu_a = K(\gamma)^{n-1}$
ρ_f = density of fluid
ρ_p = density of particle
τ_w = wall shear stress, $\tau_w = D\Delta p/4L$
χ = fraction of eddies with velocities exceeding hindered settling velocity of particles

Subscripts

D = deposition
exp = experimental
s = resuspension
T = transition

Literature Cited

Davies, J. T., "Calculation of Critical Velocities to Maintain Solids in Suspension in Horizontal Pipes," *Chem. Eng. Sci.*, **42**, 1667 (1987).

Dodge, D. W., and A. B. Metzner, "Turbulent Flow of Non-Newtonian Systems," *AIChE J.*, **5**, 189 (1959).

Durand, R., "Hydraulic Transport of Coal and Other Materials in Pipes," *Colloq. of Nat. Coal Board*, London (Nov., 1972).

Kao, T. Y., and D. J. Wood, "Incipient Motion of Solids in Solid-Liquid Transport System," *Trans. Soc. Min. Engrs.*, AIME, **255**, 39 (1974).

Newitt, D. M., M. A. Richardson, and R. B. Turtle, "Hydraulic Conveying of Solids in Horizontal Pipes," *Trans. Instn. Chem. Engrs.*, **33**, 79 (1955).

Oroskar, A. R., and R. M. Turian, "The Critical Velocity in Pipeline Flow of Slurries," *AIChE J.*, 550 (July, 1980).

Satchwell, R. M., M. P. Sharma, and R. L. Miller, "A Mathematical Model for Predicting Concentration Profiles in Liquid-Solid Fine Slurry Pipe Flows," *J. Energy Res. Tech.*, 141 (Sept. 1988).

Spells, K. E., "Correlations for Use in Transport of Aqueous Suspensions of Fine Solids through Pipes," *Trans. Instn. Chem. Engrs.*, **33**, 79 (1955).

Turian, R. M., and T. F. Yuan, "Flow of Slurries in Pipelines," *AIChE J.*, **23**, 232 (1977).

Wasp, E. J., J. P. Kenny, and R. L. Gandhi, "Solid-Liquid Flow-Slurry Pipeline Transportation," *Series on Bulk Materials Handling*, Trans. Tech. Publ., Rockport, MA (1977).

Zandi, I., and G. Govatos, "Heterogeneous Flow of Slurries in Pipelines," *J. Hydr. Div.*, ASCE, **93**, HY3, 145 (1967).

Manuscript received Nov. 20, 1989, and revision received Apr. 15, 1991.